Electric fields induce reversible changes in the surface to volume ratio of micropipette-aspirated erythrocytes

Christopher Katnik and Richard Waugh
Department of Biophysics, University of Rochester, School of Medicine and Dentistry, Rochester, New York 14642

ABSTRACT Micropipette-aspirated erythrocytes exhibit reversible changes in sphericity (surface-to-volume ratio) in response to applied electric fields. The potentials were applied between the shaft of the pipette and the bathing medium using Ag-AgCl electrodes and current clamping electronics. The change in surface-to-volume ratio is evidenced as a reversible change in the length of the cell projection in the pipette at constant aspiration pressure and changing voltage. The magnitude of the changes decreased in proportion to the inverse of the solute concentration indicating that the change in sphericity was due to a change in cell volume. Reversible changes in projection length equivalent to a 10% change in cell volume were observed to occur over times on the order of 10 s. The magnitude and time course of the effect were not affected by the removal of intracellular hemoglobin or inhibition of anion exchange. The effect was reduced by the presence of lanthanum and other multivalent cations in the suspending solution, suggesting that surface charge may play a role in mediating the effect.

INTRODUCTION

The interactions of electric fields with living cells and the effects of electric fields on cellular properties are important factors in a variety of phenomena. These topics have received increasing attention as a result of the implementation of electrofusion (17) and electroporation (7) in biotechnology. Of particular interest is the influence of electric fields on the mechanical stability of the cell membrane and possible synergistic effects of electric fields and mechanical stress (10). The discovery of stretch-sensitive channels in membranes has established a connection between mechanical stress and the electrical properties of the membrane (11). In the present study we set out to determine what effects electric fields might have on the physical properties of the erythrocyte.

The red blood cell has served as a model system for studying both the mechanical behavior of biological membranes and the transport of ions and water across the membrane (2, 12). Mechanically, the membrane can be modeled as a two-dimensional material with a large resistance to changes in surface area and low shear rigidity (resistance to in-plane deformation at constant area) (2). With regard to the movement of materials across the membrane, it has long been recognized that the red blood cell behaves as a nearly perfect osmometer (5). Its volume changes passively in response to changes in the tonicity of the suspending medium and the fractional change in cellular volume is proportional to the fractional change in solute concentration (12). The red cell membrane possesses a low cation permeability which, in conjunction with the Na,K-ATPase produces an asymmetric transmembrane distribution of Na^+ and K^+. It is the balance between the leak of cations and the pumping of cations by the Na,K-ATPase that provides the mechanism by which the red cell regulates its volume (16). The exchange of anions across the membrane occurs very rapidly via the anion transport protein capnophorin (band 3). However, because the permeability of the membrane to the net transport of anions is small, the membrane conductivity is relatively low (8, 15).

Two powerful and widely used techniques for determining the mechanical and transport characteristics of cell membranes are micropipette aspiration (2) and patch clamp (6) of single cells. To assess mechanical function, aspiration pressures are applied to the surface of the cell to produce force resultants (tensions) in the plane of the membrane which in turn produce deformations of the surface. Knowing the forces applied and analyzing the subsequent deformations one can compute the coefficients that characterize the mechanical behavior of the membrane. Patch clamp electronics make it possible to apply well-defined currents and voltages to a small region of the cell surface and to monitor its response. Changes in membrane conductance in response to different agonists can be readily assessed.

In the present study, we combine the high resolution optics and precisely measured pressures (used to assess mechanical function) with precision electronics (used in electrophysiological studies) to assess the influence of electric fields on cellular geometry. We find that the application of electric fields to red cells aspirated into

0006-3495/90/04/865/11 $2.00

micropipettes at fixed pressure produces significant, reversible changes in the surface-to-volume ratio of the cell. We attribute these changes to reversible, field-induced changes in the cell volume.

MATERIALS AND METHODS

Preparation of membrane systems

Normal human red blood cell membranes

Human red blood cells were obtained from healthy donors by either finger prick or by venipuncture (heparin). Cells obtained by venipuncture were separated from the plasma and the buffy coat was removed. The cells were washed three times in 300 mOsmol phosphate buffered saline (300 PBS) (128 mM NaCl, 20 mM Na_2HPO_4, 6.2 mM KH_2PO_4, 0.01 mM NaN_3, pH 7.4). Cells were resuspended in filtered, degassed 140 PBS (300 PBS diluted to 140 mOsmol with distilled water) containing 0.5% bovine serum albumin (BSA). The lower osmolarity caused the cells to swell until nearly spherical.

Nystatin treated human red blood cell membranes (high salt)

To increase the intracellular concentration of ions, cells were treated with the drug nystatin according to a modified version of Dalmark's procedure (1, 5). The red cells were washed three times in 300 mOsmol Hepes buffered saline (300 HBS) (140 mM KCl, 24 mM sucrose, 20 mM Na-Hepes [*N*-2-hydroxyethlypiperazine-*N'*-2-ethane-sulfonic acid], 9 mM KH_2PO_4, pH 6.9) and resuspended at a final hematocrit of 50%. 3 ml of the cell suspension were added to 15 ml 300 HBS containing 37.5 μg/ml nystatin (Sigma Chemical Co., St. Louis, MO; stock freshly prepared at 2.5 mg/ml in methanol). The cells were incubated at 0°C for 30 min then resuspended in 400 HBS (300 HBS plus 50 mM NaCl) and incubated again in the presence of nystatin at 0°C for 10 min. This procedure was repeated with similar incremental increases in salt concentration until a desired tonicity was reached. After removal of the final supernatant the cells were washed five times with isotonic HBS containing 0.5% BSA at 37°C. For the experiment the cells were resuspended in hypotonic PBS with 0.5% BSA.

Nystatin treated human red blood cell membranes (high sucrose)

Cells were treated in the same manner as above except that the concentration of nystatin was reduced from 37.5 μg/ml to 8.0 μg/ml, the incubation times were increased from 10 to 30 min, and sucrose rather than NaCl was used to increase the tonicity of the final suspending medium.

DIDS treated, sulfate loaded HRBC's

Cells were treated with anion exchange inhibitor DIDS (4,4'-diisothiocyanostilbene-2,2'-disulfonate) according to the procedure of Knauf et al. (8). 2 ml of packed cells were suspended in 40 ml of 300 mOsmol S buffer (110 mM K_2SO_4, 5 mM Na-Hepes, pH 7.5), and incubated at 37°C for a total of 2 h with buffer changes at 30 min intervals. After washing, 0.15 ml packed cells were suspended in 4.5 ml S buffer containing 25 μM DIDS and incubated at 37°C, in the dark, for 30 min. For the experiment, cells were dispersed into 150 mOsmol S buffer containing 0.5% BSA.

To test the effectiveness of the DIDS treatment, the rate of chloride influx was measured for the sulfate-loaded cells and for the sulfate-loaded DIDS-treated cells. (These measurements were performed in the laboratory of Dr. P.A. Knauf, Rochester, NY.) Cells were suspended at 3% hct (vol/vol) in 300 PBS containing 300 μCi/ml ^{36}Cl and incubated for periods of 1.5–240 min. Samples (0.5 ml) were added to 1.5 ml Drabkins solution for hemoglobin determination. The cells were separated from the suspending buffer by centrifugation through a layer of silicon oil, and the pellets were extracted in 5% trichloroacetic acid. The amount of ^{36}Cl in the extract was determined by scintillation counting. The counts per minute of the sample (C) were recorded as a function of the incubation time. For the sulfate-loaded cells (not treated with DIDS) the half time for influx was ~15 min and it was possible to measure the equilibrium counts (C_∞^S) directly (the mean of the 90 and 120 min incubation times). For the DIDS-treated cells, the halftime for influx was too long and thus it was impossible to measure the equilibrium counts (C_∞^D) directly. However, C_∞^D could be calculated from C_∞^S recognizing that the counts at steady state are proportional to the number of cells sampled (which is proportional to the hemoglobin concentration [Hb]) and the counts/min of the suspending buffer (C_s):

$$C_\infty^D = \frac{(C_s[Hb])_D}{(C_s[Hb])_S} \cdot C_\infty^S, \tag{1}$$

where subscript D denotes values for DIDS-treated sulfate-loaded cells and subscript S denotes sulfate-loaded cells (not treated with DIDS). The time constant for influx, k, is calculated by linear regression to:

$$\ln\left(\frac{C_\infty}{C_\infty - C}\right) = kt, \tag{2}$$

where C is the counts/min at time t. Note that because chloride-chloride exchange is much faster than chloride-sulfate exchange if any chloride were left inside the cells after sulfate loading, there would be an initial rapid influx of ^{36}Cl which would appear as a nonzero intercept in the curve described by Eq. 2. ("Trapped" extracellular fluid would also result in a nonzero intercept, so the intercept provides an upper bound for the amount of chloride inside the cell.) The data for the sulfate-loaded cells indicated that the residual chloride concentration after loading was <7.0 μM.

Red cell ghost membranes

Red blood cell ghosts were prepared by a modified version of the protocol of Schwoch and Passow (13). The red cells were washed in 300 PBS pH 6.0 until the supernatant stabilized at pH 6.0. 3 ml of a 50% cell suspension were added to 30 ml lysing solution (1.0 mM EDTA [ethylenediamine tetraacetate], 6.0 mM NaCl, 10 nM PMSF [phenylmethylsulfonyl fluoride], 1.0 mM ATP) at 0°C. The pH was adjusted to pH 6.0 with ice cold acetic acid. The cells were incubated at 0° for 5 min then separated from the suspending medium by centrifugation (19,000 g) at 0°C. The membranes were resuspended in 50 ml ice cold resealing solution (165 mM KCl, 59.5 mM TRIS [tris-hydroxymethyl aminomethane], 3.0 mM ATP, 0.175 mM $MgCl_2$, and 100 μM PMSF). After 10 min at 0°C, the membranes were incubated at 37°C for 45 min, allowing the membranes to reseal. The resealed membranes (ghosts) were washed once with 300 PBS and dispersed into 140 PBS containing 0.5% BSA for measurement.

Apparatus

Micropipettes

Micropipettes were made from capillary tubing (Kimax 0.9 mm OD × 0.2 mm Wall; Glass Company of America, Bargaintown, NJ) pulled to a needle point. The tip of the needle was fractured off squarely with a microforge. The completed pipettes were filled with filtered buffer solution which was isotonic to the cell-suspending medium, but which contained no BSA.

Microscope chambers

Chambers used to view the suspended cells on the microscope were constructed from glass microscope slides cut and epoxied to form a 15 × 15 × 3 mm well. The chamber was completed by sealing a siliconized coverslip to the bottom of the well with vacuum grease.

Optics

Experiments were performed on an inverted microscope (model M; Nikon Inc., Garden City, NY). The microscope was equipped with a trinocular head allowing simultaneous viewing by the operator and recording of the image on videocassette (AG6300; Panasonic, Secaucus, NJ) via a television camera (model TC1005/N; RCA, Lancaster, PA). For red cell work, a 40× objective and monochromatic brightfield illumination (436 nm) were used. When working with ghosts, the monochromatic filter was removed and Hoffman modulation contrast was used. A stage micrometer was photographed during each experiment for distance calibration

Aspiration pressure

Hydrostatic pressure gradients were generated across the tip of the pipette via a water reservoir connected to the pipette via a continuous fluid pathway. A pressure transducer (Validyne Engineering Corp., Northridge, CA) was used to monitor the applied pressure.

Electrical system

Potentials were applied across two Ag-AgCl electrodes, one at the base of the pipette and one in the bathing medium (chamber), using current clamping electronics (modules S-7100A and S-7071A; World Precision Instruments Inc., New Haven, CT). The chamber electrode was ground. This system was capable of setting a zero baseline voltage, injecting a constant current, and monitoring both the current and voltage between the electrodes. Because the device injected a fixed current, it was necessary to adjust for temporal drift in the potential manually. The magnitude of the drift was never more than 10 mV during the course of a measurement. The microscope stage and the hydraulic lines entering the stage area were electrically shielded in a grounded Faraday cage. AC noise was monitored with an oscilloscope (Tektronix Inc., Beaverton, OR) and maintained at <1.0 mV.

Measurements and calculations

Cells swollen in hypotonic media were aspirated into a micropipette with sufficient aspiration pressure to draw the outer portion of the cell into a sphere (Fig. 1). Changes in projection length were measured as a function of applied voltage at constant aspiration pressure. The pressure was held constant at either 1 or 6 cmHg (for some fragile cells the higher pressure had to be reduced to 4 or 5 cmHg) and the voltage was increased stepwise in increments of 250 mV from 0.0 to ±1,000 mV. The outer cell diameter was measured at zero volts and the length of the projection in the pipette was measured at each voltage.

The surface area and volume of a cell aspirated into a micropipette are given by simple geometric expressions:

$$A = \pi(4R_o^2 - R_p^2 + 2R_pL) \qquad (3a)$$

$$V = \pi/3(4R_o^3 - R_p^3 + 3R_p^2 L), \qquad (3b)$$

where L is the length of the projection in the pipette, R_o is the radius of the part of the cell outside the pipette, and R_p is the inner radius of the pipette at the tip. Changes in either the area or volume of the cell were observed as changes in the length of the projection in the pipette. Changes in the outer radius R_o also occurred, but were too small to be resolved optically. The change in projection length can be expressed unambiguously as a change in the sphericity (S) of the cell:

$$\Delta S \simeq S[2\pi R_p(2R_p/6V_o - 1/A_o)\Delta L], \qquad (4)$$

where S is defined as,

$$S = \frac{4\pi}{(4\pi/3)^{2/3}} \cdot \frac{V^{2/3}}{A}, \qquad (5)$$

V_o is the initial cell volume (volume at 0 mV) and A_o is the initial cell surface area. If the change in cell volume, ΔV, is known, the change in cell area, ΔA, corresponding to a change in projection length, ΔL, can be calculated by:

$$\Delta A \simeq 2\pi R_p \Delta L(1 - R_p/R_o) + 2\Delta V/R_o. \qquad (6)$$

Conversely, if the change in area is known, the change in volume can be calculated:

$$\Delta V \simeq \pi R_p^2 \Delta L(1 - R_o/R_p) + R_o\Delta A/2. \qquad (7)$$

In practice, the total length change that is observed includes the length change mediated by the applied field as well as a gradual change in the resting length of the projection. (This gradual change can be thought of as a drift in the reference geometry of the cell.) The mechanism for this drift is not known. It may be due to a gradual loss of cations from the cell or a slight increase in the osmolarity of the suspending medium due to evaporation of the suspending solution. The gradual change is approximately linear in time so that its contribution to the total change in projection length can be estimated by interpolation. The resting length is measured at the beginning (L_i) and end (L_f) of each measurement sequence. The resting (reference) length at time t is calculated by interpolation and subtracted from the total length at time t (L_t) to obtain the field-induced change in length: $\Delta L = L_t - L_o(t)$, where

$$L_o(t) = L_i + (L_f - L_i)\frac{t - t_i}{t_f - t_i}, \qquad (8)$$

where t_i and t_f are the times at which L_i and L_f were measured.

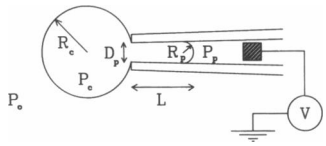

FIGURE 1 Schematic representation of a micropipette-aspirated cell. The cell was osmotically swollen until nearly spherical. A negative pressure ($P_p - P_o$) applied to the back of the pipette draws the cell into the pipette a length L. Because the interior pressure of the cell P_c is greater than the exterior pressure P_o, the portion of the cell exterior to the pipette is spherical with radius R_o, and the edge of the cell projection inside the pipette is hemispherical with radius R_p (the inner diameter of the pipette D_p is optically measured at its tip and is assumed to be constant along the length of the cell projection).

RESULTS

Red cells aspirated at a constant pressure exhibited changes in the length of the projection in the pipette, L,

upon application of an electric potential, ϕ between the pipette and chamber electrodes (Fig. 2). The direction and magnitude of the changes in projection length depended on the polarity of the applied voltage. Negative potentials produced linear increases in projection length that were larger than the decreases produced by positive potentials, and at large positive potentials the effect appeared to saturate (Fig. 3). The time course of a change in projection length in response to a step change of -1.0 V across the cell is shown in Fig. 4. The reversibility of the process is demonstrated by the return of the projection to its original length when the voltage was turned off. The time course of both the response and the return to the original length were exponential with a time constant determined by least squares regression of ~3.3 s. It should be emphasized that the potential reported here is the applied potential and not the potential across the cell itself. It was impossible to calculate the potential across the cell because of the small magnitude and anomalous behavior of the resistance of the "seal" between the cell and the pipette (see Appendix A).

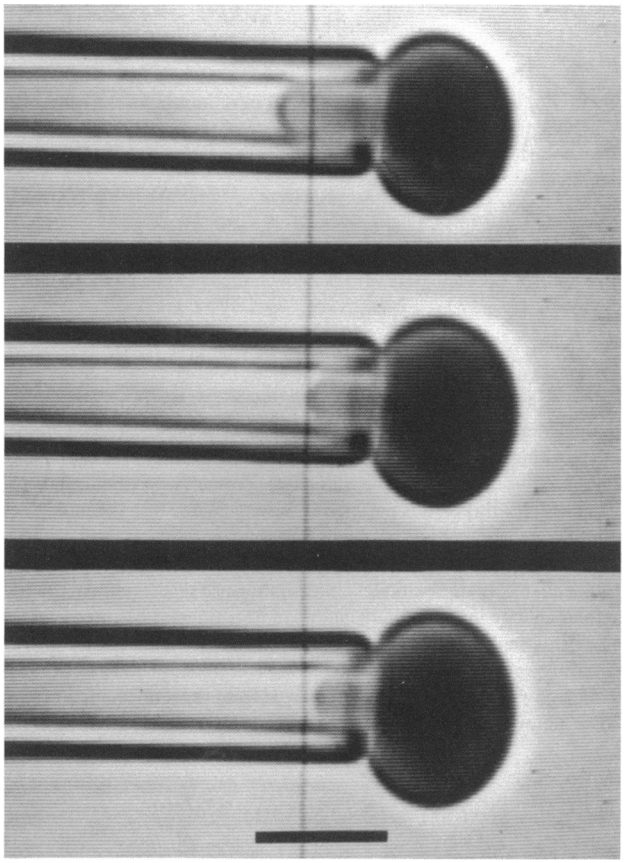

FIGURE 2 Photographs from a televison monitor showing the changes in projection length of an aspirated cell with changes in applied voltage. The applied potentials are -1.0 (*top frame*), 0.0 V (*middle frame*), and $+1.0$ V (*bottom frame*). These observations were made over a period of ~1.0 min. The aspiration pressure was constant (5.0 cmHg). The cursor marks the tip of the projection at 0.0 V. (Bar, 5.0 μm).

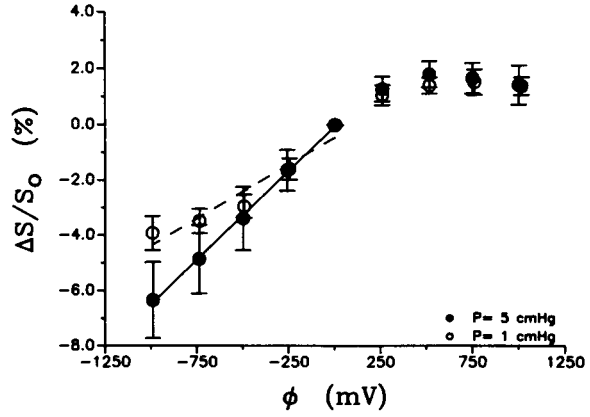

FIGURE 3 Changes in projection length expressed as fractional changes in sphericity as a function of the potential applied across the pipette and chamber electrodes. Closed circles represent means of twenty cells aspirated at a constant pressure of 5 cmHg. The solid curve is the linear regression to the data for negative voltages. Open circles represent means of 20 cells aspirated at a constant pressure of 1 cmHg. The dashed curve is the linear regression to the data for negative voltages. Error bars represent plus or minus one standard deviation of the sample means. The empty pipette resistance (resistance between the electrodes without a cell aspirated into the pipette tip) was 150 MΩ.

The magnitude of the change in sphericity with applied voltage was found to decrease in proportion to the inverse

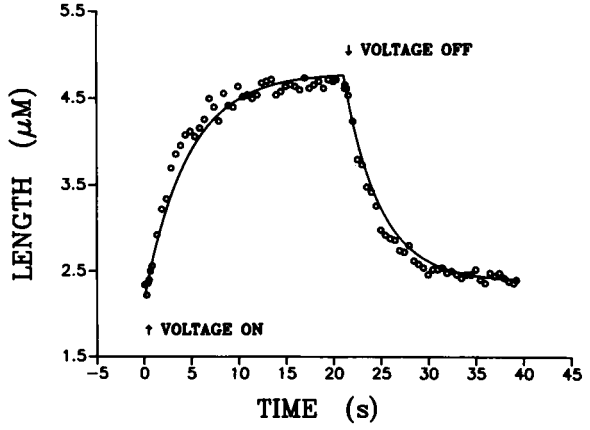

FIGURE 4 Time course of the change in the projection length in response to a step change in voltage. The aspiration pressure was constant (2 cmHg). At time zero, a potential of -1.0 V was applied across the electrodes. After 21s the potential was turned off. Points represent projection length measurements taken at 0.5 s intervals. The solid curves are first order exponentials [$L = L_f - (L_f - L_o)e^{-t/\tau}$, and, $L = L_o + (L_f - L_o)e^{-t/\tau}$] determined from the data by least squares regression. The time constants for both extension and recovery were ~3.3 s.

of the solute concentration (Fig. 5). This occurred at both high and low aspiration pressures and whether salt or sucrose was used to increase the suspending solute concentration. This is illustrated in Fig. 6, in which the slopes of the sphericity vs. negative potential data are plotted as a function of inverse concentration. The change in sphericity with positive potential was similarly reduced with increasing solute concentration.

Removal of hemoglobin from the cell had no significant effect on the response of the cell to the applied fields. Based on the dilution at lysis, we estimate that the hemoglobin concentration within the ghost membranes was <8.0% of that in intact cells, but the fractional change in sphericity with applied voltage (Fig. 7) and the time course of the response were nearly identical to that observed in the intact cell.

Similarly, neither the magnitude nor the time course of the response were affected by inhibition of anion exchange across the membrane. The behavior of sulfate-loaded cells treated with the inhibitor DIDS was indistinguishable from untreated cells. Measurements performed on 10 cells (results not shown) gave mean values for the fractional change in sphericity per negative volt of 8% (5 cmHg aspiration pressure) and 4.5% (1 cmHg aspiration pressure). (Values for untreated cells were 6 and 4%, respectively.) The response time of the DIDS-treated cells to step changes of ±10 V was <20 s, similar to that of normal red cells. The cells were tested to determine the extent of inhibition of anion exchange. For cells with intracellular chloride replaced with sulfate the half time for chloride-sulfate exchange was calculated to be 15.2 min, and for sulfate loaded cells treated with DIDS the half-time was calculated to be 280.5 min.

The presence of multivalent cations in the suspending medium caused a significant reduction in the magnitude

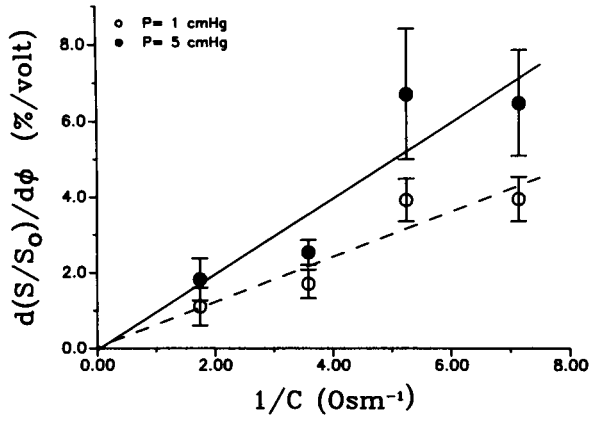

FIGURE 6 Fractional changes in sphericity per applied negative potential as a function of the inverse of solute concentration of nystatin-treated cells. Open and closed circles represent the slopes of the linear fits of fractional sphericity changes versus negative potential for cells aspirated at 1 cmHg and 5 cmHg, respectively. The dashed line is the linear regression to the data obtained at 1 cmHg aspiration pressure. The solid line is the linear regression to the data at 5 cmHg. Error bars represent the 95% confidence limits calculated for the slopes using a Student *t*-test.

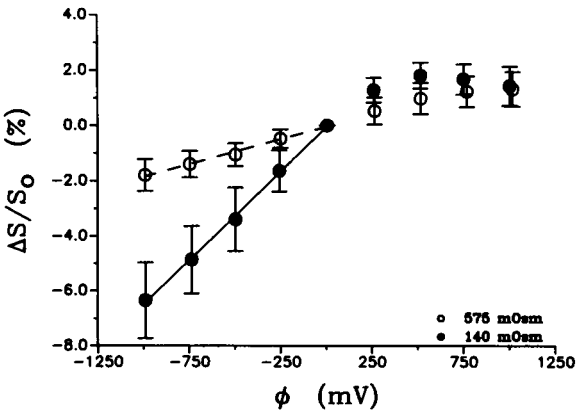

FIGURE 5 Changes in projection length of nystatin-treated cells expressed as fractional changes in sphericity as a function of the potential applied accross the pipette and chamber electrodes. The aspiration pressure was 5 cmHg. Closed circles represent means of 20 nystatin treated cells suspended in 140 mOsmol PBS. The solid curve is the linear regression to the data for negative voltages. Open circles represent means of 20 nystatin treated cells suspended in 575 mOsmol PBS. The dashed curve is the linear regression to the data for negative voltages. Error bars represent plus or minus one standard deviation of the sample means. The empty pipette resistances were 42.0 MΩ for the 140 mOsmol measurements and 13.5 MΩ for the 575 mOsmol measurements.

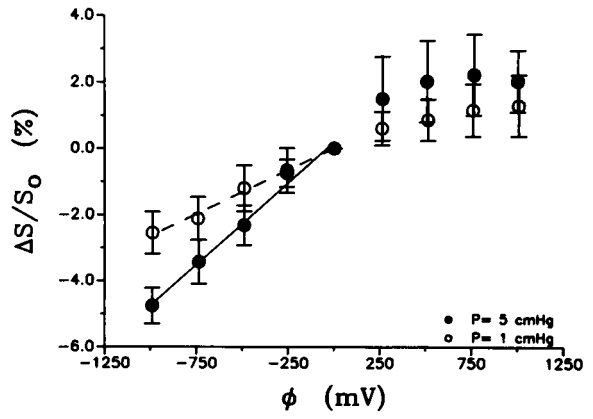

FIGURE 7 Fractional change in sphericity of red cell ghosts as a function of applied voltage. Open and closed circles represent means of five cells aspirated at a constant pressure of 1 cmHg and 5 cmHg, respectively. The lines represent the linear regressions to the data for negative voltage at 5 cmHg (*solid*) and 1 cmHg (*dashed*). Error bars represent plus or minus one standard deviation of the sample means. The empty pipette resistance was 60 MΩ.

of the cellular response to applied fields. The chloride salts of manganese, cobalt, and lanthanum were tested. Of these, lanthanum was the most effective at reducing the cellular response. The effect was completely eliminated at a lanthanum concentration of 400 μM (Fig. 8). Cobalt and manganese also reduced the response, but required higher concentrations to produce a noticeable reduction. At a $CoCl_2$ concentration of 9.0 mM the change in sphericity per volt at 5 cm Hg aspiration pressure and negative voltage applied was ~0.8%/V, and at a $MnCl_2$ concentration of 13.7 mM, the change in sphericity was ~1.7/V. These concentrations were chosen because they are the charge-reversal concentrations for these ions determined by Seaman and Pethica (14). Compare these values to a change in sphericity of 7.0%/V when no polyvalent cations are present and ~0.0%/V in the presence of 0.4 mM $LaCl_3$.

DISCUSSION

These observations demonstrate that electric fields applied across micropipette-aspirated cells have a significant effect on the cellular geometry. In assessing the mechanism for this effect, we are hampered by the inherent limitation of the micropipette technique that one

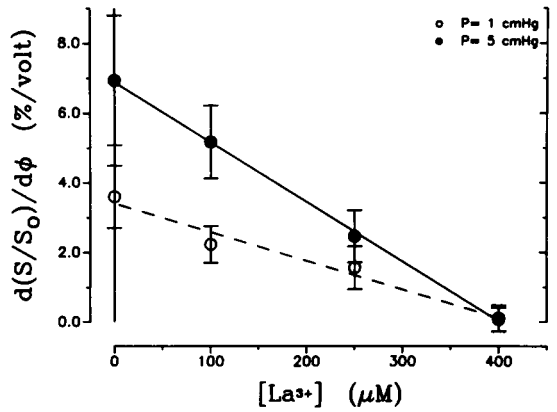

FIGURE 8 Fractional sphericity changes per applied negative potential as a function of lanthanum concentration. Circles represent the slopes of the linear fits of fractional sphericity changes versus applied potential for cells subjected to negative potentials. Closed circles represent the slopes of the linear fits of fractional sphericity changes versus applied potential for cells aspirated at a constant 5 cmHg pressure. The open circles represent slopes calculated for cells aspirated at 1 cmHg. The dashed line is a linear regression to the slopes calculated for cells aspirated at a constant 1 cmHg. The solid line is a linear regression to the slopes calculated for cells aspirated at a constant 5 cmHg. Error bars represent 95% confidence limits calculated for the slopes using a Student t-test. The empty pipette resistance was 74 MΩ for the 0.0-μM measurements, 74 MΩ for the 100-μM measurements, 76 MΩ for the 250-μM measurements, and 73 MΩ for the 400-μM measurements.

cannot distinguish directly between changes in surface area and changes in volume. This limitation arises because changes in the outer radius of the cell are too small to be resolved optically. Thus, changes in only one geometric parameter (L) can be detected accurately. Consequently, the change in surface area or volume cannot be calculated without estimating the change in R_o by applying an additional constraint. Thus, to calculate the change in surface area it is necessary to know what is happening to the cell volume, or to calculate the change in volume is necessary to make assumptions about the surface area.

The magnitude of the changes in projection length and the dependence of the effect on solute concentration lead to the conclusion that much, if not all of the change in sphericity is due to a change in cell volume. The largest changes in projection length observed would require area dilations of ~10%, far in excess of what is thought to be the maximum change that the cell membrane can sustain without lysis (3–4%) (3, 4). Therefore, the change in sphericity must be due at least in part to a change in cell volume.

A change in cell volume requires a movement of water across the cell membrane. Application of the electric field must cause a change in the chemical potential of the water within the cell. In response to this change, water will move down its potential gradient until a new steady state is reached. The main contributors to the chemical potential of the water (μ_w) are the hydrostatic pressure and the concentration of solutes. In dilute (ideal) solutions:

$$\mu_w = \mu_w^o - RT\sum_i C_i + \bar{v}P, \qquad (9)$$

where the summed term represents the total concentration of solutes, RT is the gas constant times absolute temperature, $\bar{v}$ is the partial molar volume of water, P is pressure relative to the standard state, and μ_w^o is the chemical potential of water in the standard state (in the absence of solute). Thus, the movement of water can be caused by either a change in solute concentration or a change in hydrostatic pressure.

The hydrostatic pressure difference across the membrane is determined by the aspiration pressure plus any mechanical forces on the cell imposed by the electric field. The magnitude and direction of the electromechanical force are uncertain. They depend on the surface charge densities of the inner pipette surface and the membrane and on how the fluid drag resulting from electroosmotic flow is distributed between the membrane and the pipette surface (Appendix B). Worst case estimates suggest that electromechanical forces may be comparable to the force of the aspiration pressure. However, there is clear evidence that electromechanical forces are not responsible

for the change in projection length we have observed. First is the observation that under conditions in which the electromechanical force is supposed to add to the aspiration pressure (negative potential applied, increasing projection length) the cells do not lyse, even when the membrane tension due to the aspiration pressure is large (~4 dyn/cm, aspiration pressure = 5 cmHg). The observation that at zero applied volts membranes begin to lyse at a membrane tension of ~6 dyn/cm indicates that any addition to the membrane tension by electromechanical forces must be <2 dyn/cm. A similar conclusion is reached by considering the situation in which electrochemical forces ought to subtract from the aspiration pressure (positive potential applied, decreasing projection length). In this case, even when the membrane tension is small (~0.7 dyn/cm), in the presence of the electric field the membrane tension remains positive and finite: the membrane does not become flaccid and the projection is not forced out of the pipette. Thus, the contribution to the membrane tension by the field must be <0.7 dyn/cm. In addition, it should be recognized that when positive potentials are applied the projection length is shorter than it would be at zero volts and zero pressure, even when the aspiration pressure is large. Clearly, electromechanical forces cannot account for the behavior we have observed.

These arguments lead to the conclusion that the volume change must be mediated by a movement of ions across the membrane in response to the electric field. At steady state, there is a difference in solute concentration across the membrane because the aspirating pipette pressurizes the cell interior (4). (This is evident from the spherical shape of the portion of the cell outside of the pipette.) Essentially, water is squeezed out of the cell because the pressure inside the cell is greater than the pressure outside. This results in an increase in the salt concentration within the cell. At steady state the net flux of water out of the cell is zero. From this condition, the difference in concentration between the cell interior (C_i) and the suspending medium (C_o) can be determined (4).

$$C_i - C_o = \frac{2\bar{T}}{RT}\left(\frac{A_p/R_p + A_o/R_o}{A_p + A_o}\right), \tag{10}$$

where $\bar{T}$ is the membrane tension, RT is the gas constant times temperature, A_p and A_o are the membrane areas in the pipette and outside the pipette, and R_p and R_o are the radii of the pipette and the spherical section of the cell outside the pipette. Thus, the solute concentration inside the cell is determined by the membrane tension and the solute concentration in the suspending medium. Assuming that these quantities ($\bar{T}$ and C_o) are not appreciably affected by the electric field, the intracellular solute concentration must be the same before and after the field is applied. Let n_1 and n_2 be the number of solute molecules in the cell before and after the field is applied, and let us further assume that $\Delta n = n_2 - n_1$, is a function of the applied potential. Constant membrane tension and constant extracellular concentration require (Eq. 10)

$$n_1/V_1 \simeq n_2/V_2, \tag{11}$$

or

$$\frac{\Delta n}{n_1} \simeq \frac{\Delta V}{V_1}, \tag{12}$$

where V_1 and V_2 are the cell volumes before and after the field is applied, and $\Delta V = V_2 - V_1$. Thus, for a given $\Delta n(\phi)$, the corresponding volume change is inversely proportional to the number of solute species in the cell, n. Our observation that the magnitude of the field-induced change is proportional to the inverse of the solute concentration (Fig. 6) is consistent with this result.

It is unlikely that the effect we are observing is mediated by a movement of cations. The normal permeability of the membrane to cations is too low to account for such a rapid change in volume (12). Even if it is postulated that the field increases cation permeability, it is difficult to explain how a loss of cations could be reversible. To reverse the process, the cations must move against their electrochemical gradient, and the capacity of the Na-K ATPase is orders of magnitude too small to move so many ions in so little time (16). Thus, the rate at which the change occurs and its reversibility exclude cation movement as a possible mechanism for the effect.

Because cations are immobile and the intracellular pressure is fixed by the aspiration pressure, we conclude that the water movement out of the cell must be mediated by a movement of anions. The fact that the response to the field is not affected by blocking anion exchange (via band 3) indicates that a net transport of ions through some other channel is involved. It is instructive to consider how rapidly such transport must occur in light of published values for the chloride permeability. For a change in cell volume of ~10%, a movement of chloride equivalent to a change in concentration of ~30 mM must occur. Thus, whatever driving force is generated by the field must be roughly equivalent to a concentration difference across the membrane of 30 mM. The flux J_{Cl} in response to such a driving force is:

$$J_{Cl} \simeq P_{Cl}(C_i - C_o), \tag{13}$$

where P_{Cl} is the permeability of the membrane for the net transport of chloride, C_i is the intracellular concentration, and C_o is the extracellular concentration. Our measurements of the time-course of the process show that the movement must occur over a period of ~10 s. Taking the volume of the cell to be ~100 μm^3 and the surface area to be ~130 μm^2, the permeability of the membrane must be

$\sim 10^{-5}$ cm/s. This is ~300 times higher than the value measured using valinomycin (12). However, another report (15) indicates that the permeability of red cells measured in bulk with valinomycin may be a lot smaller than the permeability observed for cells aspirated into glass capillaries. Using a glass microelectrode to measure chloride conductance in red cells from *Amphiuma*, Stoner and Kregenow (15) found a value of 20–100 times greater than the conductance measured using valinomycin in those cells. Our conclusion that there is a (relatively) rapid flux of chloride out of the cell is consistent with Stoner's measurements of high chloride conductivity in pipette-aspirated erythrocytes.

Although movement of water in concert with a movement of anions provides a plausible explanation for the effect we have observed, the details of the underlying mechanism remain obscure. One possibility is that there is a change in intracellular pH caused by the field, resulting in a change in the ionization of impermeant intracellular buffers (e.g., hemoglobin). Freedman and Hoffman (5) have investigated the dependence of hemoglobin ionization on pH. According to their findings, a change in the charge concentration of hemoglobin of 20 mM will occur for a change in intracellular pH of ~0.25 pH units. The persistence of the effect in ghosts may be explained by the presence of residual hemoglobin and other impermeant buffers within the ghost cells.

The dependence of projection length on potential was linear for negative voltages, but appeared to saturate at large positive voltages (Fig. 4). Even at the highest positive voltage, the length of the projection was greater than the pipette radius, indicating that the saturation of projection length changes at positive voltages is a characteristic of the mechanism responsible for the effect and not a consequence of the cellular geometry. However, the significance of this characteristic of the effect is not clear.

Although the precise mechanism responsible for the effect is not known, its inhibition by micromolar concentrations of lanthanum indicates that surface charge may be an important factor in the process. The effect of the electric field is completely eliminated at a lanthanum concentration of 0.4 mM. This is the concentration determined by Seaman and Pethica (14) to be the charge reversal concentration for the electrophoretic mobility of red cells. Alternatively, La^{3+} may reduce the effect of the field by affecting the permeability of other ionic species either by direct interaction with the channels or indirectly via an effect of lipid organization.

The presence of cobalt or manganese in the suspending buffer also reduced the effect of applied fields on the cell volume, but these ions were not as effective as lanthanum at eliminating the effect. It appeared that the higher the charge reversal concentration for a particular cation, the less effective that cation was at reducing the effect of the field. Seaman's determination of charge reversal concentrations for these cations was based on electrophoretic mobility. In this case, the surface charge is neutralized at the "shear plane." It is possible that in the present study it is necessary to neutralize the charge at a different plane in the vicinity of the surface, e.g., the Stern layer, and that cobalt and manganese simply have a lower affinity for the surface.

The observation that polyvalent ions reduce the effects of the field raised the possibility that the reduction of the effect in high salt concentration might have been due to the increase in ionic strength and consequent shielding of the surface charge. However, subsequent measurements performed at constant external salt concentration with sucrose used to increase the osmolarity of the suspending medium to the appropriate level confirmed that it was the increase in solute concentration that reduced the change in cellular volume, and not shielding of external of surface charge by high ionic concentrations (results not shown).

CONCLUSIONS

These results indicate that the electric field–induced deformations of micropipette-aspirated red cells are due to reversible changes in cellular volume. These volume changes depend on the magnitude and polarity of the applied field. The effect is not mediated by anion exchange. Conditions under which the effect is minimized include addition of 0.4 mM La^{3+} to the suspending medium and increasing the suspending solute concentration. A change in the ionization of hemoglobin caused by the applied field is a possible mechanism for the effect. The details of such a mechanism have not been resolved but increased membrane permeability to chloride and effects of applied fields on intracellular pH may be implicated. The magnitude of the effect is significant, and investigators should be aware of possible erroneous interpretation of measurements obtained when electric fields in micropipettes are not adequately controlled.

These studies have raised a number of important issues about the transport of ions across the red cell membrane that are outside the original scope of the study. These indicate possible effects of membrane tension and/or the proximity of a glass surface on chloride premeability and intracellular pH. In addition, the anomalous decrease (!) in electrical resistance when cells are aspirated at negative voltages remains unexplained. The mechanisms underlying these phenomena may have general importance in the interpretation of electrophysiological studies, and we look foward to their future delineation.

APPENDIX A

Potentials reported in the present work are those applied between the electrode in the pipette and the electrode in the chamber (ground). It was not possible to calculate the potential drop across the cell itself because of anomalous changes in resistance that were observed when negative currents were applied. Ordinarily, the potential across the cell could be calculated using a simple voltage divider model and measurement of the empty pipette resistance, the pipette resistance with an aspirated cell, and the potential applied across the electrodes. However, when the applied potential was negative, the apparent resistance between the electrodes decreased when a cell was aspirated into the pipette tip and decreased further as the aspiration was increased. Fig. A1 shows the voltage required to produce a given current at several different aspiration pressures. The solid line shows the voltage-current dependence in the absence of an aspirated cell. Note that at negative voltages less voltage is required to produce the same current when there is a cell in the pipette tip than when the pipette is empty. This effect depended on the empty pipette resistance. As the pipette geometry was modified to lower its resistance from 100–200 MΩ to 10–50 MΩ the magnitude of the decrease in resistance changed from ~ −30% to ~0% (Figs. A1 and A2). With all the pipettes examined, the resistance, as measured with positive currents, always increased upon aspiration of a cell and the increase was greater as the pressure was increased. This anomalous behavior was verified using voltage clamp apparatus in another laboratory. Using the resistance change measured for positive voltages we estimate that ~10% of the applied potential falls across the cell itself.

APPENDIX B

In this appendix the importance of electromechanical forces is considered. There are two main contributions to the force on the cell from the field: electrophoretic and electroosmotic. To evaluate the magnitude of these contributions we consider the cylindrical region of the cell projection where the membrane is in close apposition to the inner wall of the pipette. The electrophoretic force results from the interaction of the field with the net negative charge on the membrane. Let the surface density of charge of the membrane be σ_m and the membrane area in the cylindrical region of contact be A_c. The electrophoretic force is:

$$f_{ph} = \sigma_m E A_c, \tag{B.1}$$

where E is the electric field. For simplicity we have assumed that both σ_m and E are constant along the region of contact. Note that the electrophoretic force acts in the direction opposite to the movement of the membrane projection that has been observed. The electroosmotic force arises from the interaction of the field with the positive counter ions near the surface of the membrane and the pipette. The force on the fluid (f_f) can be thought of as a body force (analogous to gravity) on the fluid. Its magnitude depends on the field strength E and the charge density in the fluid, ρ_c. Although an exact calculation of the force is complex, an estimate can be made if we assume that the electric field and the charge density of the fluid between the membrane and the pipette are uniform. The total force on a volume of fluid V is then:

$$f_f = \rho_c V E. \tag{B.2}$$

At steady state there is a constant flow of fluid in the gap. The balance of forces requires that the body force, f_f, be equal and opposite to the sum of the forces from shear stress on the fluid exerted by the membrane (τ'_m) and by the wall of the pipette (τ'_p):

$$f_f + \tau'_m A_m + \tau'_p A_p = 0, \tag{B.3}$$

where A_m and A_p are the areas of the membrane and the pipette in the region of contact. The total force on the membrane ($\tau_m A_m = -\tau'_m A_m$) from electroosmosis is

$$f_{os} = \tau_m A_n = \rho_c V E - \tau_p A_p. \tag{B.4}$$

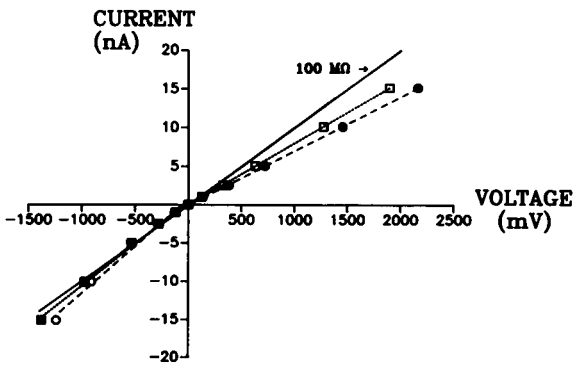

FIGURE A1 Voltage-current relationships for the circuit with an aspirated cell using a "high" impedence micropipette. Closed circles represent the circuit behavior with a cell aspirated at 6 cmHg with positive current injected. Open squares represent the circuit with a cell aspirated at 1 cmHg and positive current injected. Closed squares represent the circuit with a cell aspirated at 1 cmHg and negative current injected. Open circles represent the circuit with a cell aspirated at 6 cmHg and negative current injected. The solid line represents the circuit without an aspirated cell (100 MΩ).

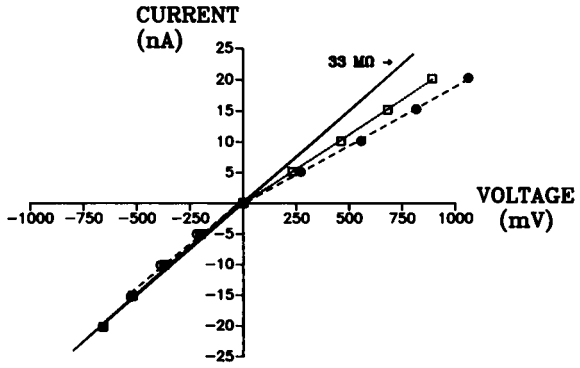

FIGURE A2 Voltage-current relationships for the circuit with an aspirated cell using a "low" impedence micropipette. Closed circles represent the circuit behavior with a cell aspirated at 3 cmHg with positive current injected. Open squares represent the circuit with a cell aspirated at 1 cmHg and positive current injected. Closed squares represent the circuit with a cell aspirated at 1 cmHg and negative current injected. Open circles represent the circuit with a cell aspirated at 3 cmHg and negative current injected. The solid line represents the circuit without an aspirated cell (33 MΩ).

Note that the force of the fluid on the pipette wall $\tau_p A_p = -\tau'_p A_p$, and that the force on the membrane acts in the same direction as the observed movement of the membrane projection.

As the limiting case for the maximum electroosmotic force, let the total positive charge in the gap be equal to the sum of the stationary negative charges on the membrane and pipette:

$$\rho_c V = (\sigma_m + \sigma_p) A_c. \tag{B.5}$$

For this case, the electroosmotic force on the membrane is:

$$f_{os} = (\sigma_m + \sigma_p) E A_c - \tau_p A_p, \tag{B.6}$$

and the net force is the quantity less the electrophoretic force (Eq. B.1):

$$f_{net} = \sigma_p A_c E - \tau_p A_c. \tag{B.7}$$

The magnitude and direction of the net force depend on what assumptions are made about relative magnitudes of fluid shear forces $\tau_m A_m$ and $\tau_p A_p$, and the charge densities σ_m and σ_p. If we assume that the surfaces of the membrane and the pipette are smooth and the distance between them is small, then the flow can be approximated as a flow between parallel plates, and we find (Eq. B.6): $\tau_m A_m = \tau_p A_p = E(\sigma_m + \sigma_p) A_c/2$. The net force per unit area becomes:

$$\frac{f_{net}}{A_c} = \left(\frac{\sigma_p - \sigma_m}{2}\right) E. \tag{B.8}$$

The magnitude and direction of the force depend on the relative magnitudes of the charge densities σ_p and σ_m. A different result is obtained if it is assumed that the region between the membrane and the pipette is filled with the glycocalyx. In this case it can be argued that the fluid drag on the membrane (including the glycocalyx) is much greater than the fluid drag on the wall of the pipette, and the term $\tau_p A_p$ (Eq. B.4) can be neglected. In this case the net force per unit area is (Eq. B.7)

$$\frac{f_{net}}{A_c} = \sigma_p E. \tag{B.9}$$

In this case the direction of the force is consistent with the movement of the projection, and depends on the charge density on the pipette glass.

It should be emphasized that these equations overestimate the inward force on the cell when negative potentials are applied. They disregard the electrophoretic force on the remainder of the membrane and overestimate the density of positive charge in the gap between the cell and the pipette. Nevertheless, they are useful for making order-of-magnitude estimates of the electromechanical force on the cell. Accurate estimates are not possible because the charge density on the pipette is not known. Estimates of σ_p made from measurements of streaming potential in the glass capillaries from which the pipettes are made indicate that it is similar in magnitude to the charge density of the red cell ($\sigma_m \simeq 4 \times 10^{-6}$ C/cm^2, [9]). Using this value, we can make a few simple calculations to estimate the possible magnitude of the force. Because of the high resistance of the pipette in the absence of the cell and the low resistance of the "seal" between the cell and the pipette (Appendix A), we estimate that the potential differences across the cell itself is ~100 mV when 1 V is applied across the electrodes. Supposing that this potential change occurs over a projection length of ~1.0 μm, we estimate the field in the region between the membrane and the pipette to be $\sim 10^3$ V/cm or or 10^{10} dyn/C. If the charge density on the glass is equal to the charge density on the cell, the model leading to Eq. B.8 gives a net force of zero, and the model leading to Eq. B.9 gives a net force/area of 4×10^4 dyn/cm^2. The additional membrane tension due to the electric field ($\bar{T}_e$) can be calculated from balance of forces:

$$2\pi R_p \bar{T}_e = \frac{f_{net}}{A_c} \cdot 2\pi R_p L, \tag{B.10}$$

where L is the length of the contact region. The example above gives a value of $\bar{T}_e$ (Eq. B.9) of 4 dyn/cm. This is a significant contribution. Although it is not sufficient to produce a change in membrane area as large as 10%, it would be expected to cause lysis when the initial membrane tension is >3 dyn/cm. The fact that lysis is not observed indicates that our estimate is too high. However, it is clear that electroosmotic forces can be significant under certain conditions.

The authors thank Dr. Philip Knauf for his helpful discussions about possible mechanisms for the cell volume change and for his assistance and support in determining the importance of anion exchange in this phenomenon. We thank Dr. Herman Passow for suggesting the experiments using DIDS and sulfate substitution. We also thank Dr. Robert Kass for the use of his equipment to verify the anomalous resistance changes observed during this study

This work was supported by the Public Health Service under grant HL31524.

Received for publication 20 March 1989 and in final form 10 November 1989

REFERENCE

1. Dalmark, M. 1975. Chloride transport in human red cells. *J. Physiol. (Lond.)*. 250:39–64.
2. Evans, E., and R. Skalak. 1980. Mechanics and Thermodynamics of Biomembranes. CRC Press, Boca Raton, FL. 1–241.
3. Evans, E., and D. Needham. 1987. Physical properties of surfactant bilayer membranes: thermal transitions, elasticity, cohesion, and colloidal interactions. *J. Phys. Chem.* 91:4219–4228.
4. Evans, E. A., and R. Waugh. 1977. Osmotic correction to elastic area compressibility measurements on red cell membrane. *Biophys. J.* 20:307–313.
5. Freedman, J. C., and J. F. Hoffman. 1979. Ionic and osmotic equilibria of human red blood cells treated with nystatin. *J. Gen. Physiol.* 74:157–185.
6. Hamil, O. P., A. Marty, E. Neher, B. Sakmann, and F.J. Sigworth. 1981. Improved patch clamp techniques for high-resolution current recording from cells and cell-free membrane patches. *Pfluegers Arch. Eur. J. Physiol.* 391:85–100.
7. Kinosita, J., Jr., and T. Y. Tsong. 1977. Formation and resealing of pores of controlled lysis in human erythrocyte membrane. *Nature (Lond.)*. 268:438–440.
8. Knauf, P. A., G. F. Fuhrmann, S. Rothstein, and A. Rothstein. 1977. The relationship between anion exchange and net anion flow across the human red cell membrane. *J. Gen. Physiol.* 69:363–386.
9. Levine, S., M. Levine, K. A. Sharp, and D. E. Brooks. 1983. Theory of electrokinetic behavior of human erythrocytes. *Biophys. J.* 42:127–135.
10. Needham D., and R. M. Hochmuth. 1989. Electro-mechanical permeabilization of lipid vesicles: Role of membrane tension and compressibility. *Biophys. J.* 55:1001–1009.

11. Sachs, F. 1988. Mechanical transduction in biological systems. *CRC Crit. Rev. Bioeng.* 16:141–169.

12. Sachs, J. R., P. A. Knauf, and P. B. Dunham. 1975. Transport through red cell membranes. *In* The Red Blood Cell. D. M. Surgenor, editor. Academic Press, New York. 613–703.

13. Schwoch, G, and H. Passow. 1973. Preparation and properties of human erythrocyte ghosts. *Molec. Cell Biochem.* 2(2):197–218.

14. Seaman, G. V. F., and B. A. Pethica. 1964. A comparison of the electrophoretic characteristics of the human normal and sickle erythrocyte. *Biochem. J.* 90:573–578.

15. Stoner, L. C., and F. M. Kregenow. 1980. A single-cell technique for the measurement of membrane potential, membrane conductance and the efflux of rapidly penetrating solutes in *Amphiuma* erythrocytes. *J. Gen. Physiol.* 76:455–478.

16. Tosteson, D. C., and J. F. Hoffman. (1960). Regulation of cell volume by active transport in high and low potassium sheep red cells. *J. Gen. Physiol.* 44:169–194.

17. Zimmerman, U. L. 1982. Electric field mediated fusion and related electric phenomena. *Biochim. Biophys. Acta.* 694:227–277.